Threshold Field Studies of Various Positive Corona Phenomena

K. E. FITZSIMMONS*
Department of Physics, University of California, Berkeley, California
(Received May 19, 1941)

Use of the oscillograph to study the discharge between confocal paraboloid electrodes in air at atmospheric pressure has given the threshold field strength at which the various positive corona phenomena begin. Some effects of humidity and of accumulated oxides in the gap are described. Current-potential curves are given which show the more prominent effects of humidity and accumulated oxides on the discharge after corona onset. From the field data it is possible to verify Meek's theory attending the formation of pre-onset streamers.

INTRODUCTION

PAPERS by Loeb,[1-3] Kip,[4,5] Trichel,[6,7] and others have indicated that streamers are an important aspect of the corona mechanism and of spark breakdown. Loeb pointed out that the streamer mechanism might be an alternative mechanism in the breakdown of plane parallel gaps, and later work of Meek[8] and Loeb[9] has shown it to be the mechanism for values of the product, pressure times gap length, greater than 200 mm×cm in air.

To establish a quantitative theory for streamer formation it was believed that data on the onset fields for corona might be of value. Before the present data were obtained, Meek had postulated a criterion for streamer formation on the basis of spark discharge theory, which was found to predict closely the breakdown potential for plane parallel gaps. It thus became urgent to determine whether or not Meek's criterion applied to streamer formation where the gap geometry gave a non-uniform field, such that streamers initiated corona at much lower potentials than were necessary for breakdown.

To obtain these needed data, it was necessary to measure the onset potentials for streamers in positive point corona with gaps of such geometry that the fields involved could be computed accurately. To this end a series of measurements was carried out with confocal paraboloid electrodes. While making these studies, the fields at which burst pulses, steady burst corona, and breakdown occurred were also measured. In the course of these investigations the first thing that manifested itself was the variabilities introduced by atmospheric conditions, notably humidity and the nitric oxides formed in dry air.

The purpose of these investigations was thus twofold. (1) To give the threshold field strength at which the various positive point corona phenomena begin and to include the newly discovered effects upon these of humidity and accumulations of oxide in the gap. (2) To compare the predictions of Meek's theory with experiment.

APPARATUS

The experiments were performed with air at atmospheric pressure in the gap. Two positive paraboloid points of focal lengths 0.009 cm and 0.019 cm were used, for most of the work, in conjunction with four hollow paraboloid electrodes of focal lengths 1, 2, 3, and 5 cm. The focal lengths of these hollow electrodes gave the effective gap lengths. The points were brass and the hollow electrodes were spun copper.

The high potential source and the method of making oscillographic as well as current and potential observations were very similar to those used by Kip.[4,5] As in Kip's work, a radioactive source was placed in the vicinity of the gap to provide ions to start the various onset phenomena.

When working with dry air in the gap, the entire electrode assembly was placed in a large grounded metal enclosure containing $CaCl_2$ as a

* Now at The State College of Washington, Pullman, Washington.
[1] L. B. Loeb and W. Leigh, Phys. Rev. **51**, 149 (1937).
[2] L. B. Loeb and A. F. Kip, J. App. Phys. **10**, 142 (1939).
[3] Leonard B. Loeb, *Fundamental Processes of Electrical Discharge in Gases* (John Wiley, 1939).
[4] A. F. Kip, Phys. Rev. **54**, 139 (1938).
[5] A. F. Kip, Phys. Rev. **55**, 549 (1939).
[6] G. W. Trichel, Phys. Rev. **54**, 1078 (1938).
[7] G. W. Trichel, Phys. Rev. **55**, 382 (1939).
[8] J. M. Meek, Phys. Rev. **57**, 722 (1940).
[9] L. B. Loeb and J. M. Meek, J. App. Phys. **11**, 438 (1940).

TABLE I. Values for onset of first bursts.

Gap δ (cm)	Potential of point V (volts)	Field at point surface X_A (volts/cm)	Ratio of field to pressure X_A/P (volts/cm/mm)	Distance from point where $\alpha=1$ a (cm)	Average $\int_0^a \alpha dx$ for all gaps	Average exp $[\int_0^a \alpha dx]$ for all gaps (ions)
		Dry air—point focal length 0.009 cm				
1	2976	7.0×10^4	92.4	0.0179		
2	3445	7.1×10^4	93.3	0.0181	1.31	4.46
3	3660	7.0×10^4	92.0	0.0178		
5	3890	6.8×10^4	90.0	0.0172		
		Moist air—relative humidity 55 percent at 20°C				
1	2280	5.4×10^4	70.8	0.0116		
2	2840	5.8×10^4	76.8	0.0133	0.62	1.86
3	3050	5.8×10^4	76.7	0.0133		
5	3515	6.2×10^4	81.2	0.0146		

drying agent. A small brushless electric fan fastened above the gap kept the air in circulation. This metal enclosure also served as a limiting space wherein humidity could be controlled and measured when moist air was desired in the gap. Water was introduced into the enclosure by means of a wick from which it was allowed to evaporate until the relative humidity reached the desired value. The relative humidity could be determined by observing a wet and dry bulb thermometer combination through glass windows.

With confocal paraboloids it was possible to calculate the fields, providing the focal lengths of the electrodes and the potential of the point were known. A solution of Laplace's equation, satisfying the boundary conditions involved, leads to the following relation:

$$X=\frac{V}{\log_e (f/F)}\cdot\frac{1}{x+f}. \qquad (1)$$

X is the field in volts/cm at a distance x cm from the end surface of the point electrode along the common axis of the two electrodes, V the potential of the point in volts, f the focal length of the point, and F the focal length of the grounded hollow electrode. It is seen that, once V is determined for a given pair of electrodes, the field at any point in the gap on the common axis can be computed. Furthermore, since $V/\log_e (f/F)$ is a constant for any particular value of V with a given pair of electrodes, the X *vs.* x curve for a given value of V will be a hyperbola. The field will fall in magnitude from a maximum at the point surface to a minimum at the outside electrode surface.

EXPERIMENTAL RESULTS

According to Kip and Trichel we may arrange the phenomena observed in positive point-to-plane corona in the order of their appearance with increasing point potential as follows: (1) small intermittent and irregular pre-onset bursts, (2) pre-onset streamers, (3) steady burst pulse corona of Trichel, (4) breakdown. In essence there is no fundamental difference in the phenomena whether confocal paraboloids or point-to-plane geometry is used. Kip[4] made measurements of fields with confocal paraboloids for the onset of steady burst corona and found the fields to be independent of gap length. He did not, however, extend his observations of this nature to include pre-onset bursts or streamers. In the present work Kip's observations were extensively confirmed, and in addition, a similar independence of gap length and starting fields was found for pre-onset bursts and streamers. This correlates the sequence of the point corona phenomena with the fields for their onset. The observations and discussions attributed to each of these phenomenon will be presented in the order of its onset as the potential of the point was slowly increased.

(1) Pre-Onset Bursts

Burst pulses begin to appear, according to the oscillograph, after the field at the point surface reaches a certain minimum value, depending upon the size of the point and the air pressure.

In the high field region near the point, Townsend's coefficient of electron multiplication α has a value large enough so that an electron which is in this region can produce ions by collision as it moves toward the point. The electrons produced in this process make up an electron avalanche. Townsend's coefficient will depend upon the ratio of field strength to pressure, and since the field increases as the point is approached, the number of positive ions produced by the electron as it moves to the point surface is given by $\int \alpha dx$ taken over the distance x through which the electron moves in reaching the point surface. An electron in a region where the ratio of field to pressure, X/P, is less than 20 volts/cm/mm Hg, contributes very little to ionization by collision as can be seen by reference to Sanders'[10] data on Townsend's coefficient.[11] Loeb and Kip have pointed out that, by use of Sanders' and Townsend's[12] data, the number of ions produced by collision in an electron avalanche can be found by graphical integration of αdx over the distance where α is appreciable and the subsequent evaluation of $\exp[\int \alpha dx]$. This was done for the case of burst onset as well as the other onset phenomena.

Table I gives the values for $\int_0^a \alpha dx$ and for $\exp[\int_0^a \alpha dx]$ for the onset of bursts in both dry and moist air. The relative humidity of the moist air was approximately 55 percent at 20°C. Owing to the rapid decrease of X with distance from the point surface, a was taken[11] as that distance where $\alpha = 1$. Curves in Fig. 1A show the average for all gaps of α *vs.* x at the onset of bursts and streamers in both dry and moist air. Figure 1B shows the corresponding X/P *vs.* x curves. The values of $\exp[\int_0^a \alpha dx]$ for bursts in dry air (4.46 electrons) and in moist air (1.86 electrons) are of the same order of magnitude and are surprisingly small. Each electron coming into the point through a distance a, makes avalanches of only 2 to 4 electrons. Thus, the pulses observed as bursts by Trichel,[6] which numbered in the order of 10^5 or 10^6 ions at least, must consist of a lateral spread of the single small avalanche processes over the point surface. The fact that Trichel observed the burst pulse corona in air at atmospheric pressure to spread over the point as a uniform glow gives confirmation to the idea of the lateral spread. A lateral spread can take place through photoionization of the gas by the photons from the avalanches. Since the high field necessary for avalanche formation exists only near the point; we can expect the glow to first confine itself to the point surface. The burst eventually chokes itself off by positive ion space charge accumulation and by statistical fluctuations.

The reduced value of $\int_0^a \alpha dx$ for the moist air, in comparison to the dry air, with the same criterion for burst pulse detection, can be ascribed only to a much richer yield of photoelectric ionization in contaminated air. This is not surprising since the ionization potentials of O_2 and N_2 are high, and photons capable of exciting them are rare. Water vapor and its dissociation

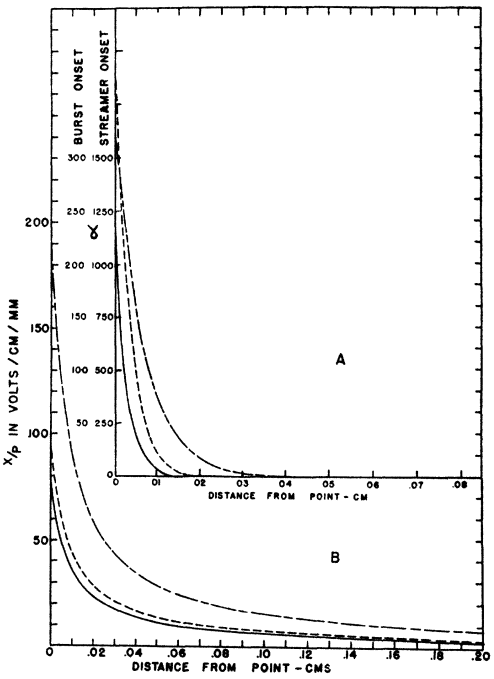

FIG. 1A. Curves showing the variation of Townsend's coefficient α with distance x from the point surface at the onset of first bursts and at the onset of streamers, in moist and dry air. Full curve represents burst onset in dry air; dotted curve represents burst onset in moist air. The dot-dash curve was plotted for streamer onset and was the same for both moist and dry air.

FIG. 1B. X/P *vs.* x curves for the onset of first bursts and for the onset of streamers. The designation given to full, dotted, and dot-dash curves in (A) applies here. Focal length of point for both (A) and (B) was 0.009 cm. Gaps of 1, 2, 3, and 5 cm were used.

[10] Frederick H. Sanders, Phys. Rev. **44**, 1020 (1939).
[11] L. B. Loeb and J. M. Meek, *The Mechanism of the Electric Spark* (Stanford Press, 1941), p. 127.
[12] J. S. Townsend, Phil. Mag. **8**, 738 (1904).

TABLE II. Values for streamer onset.

Gap δ (cm)	f (cm)	V (volts)	X_A (volts/cm)	X_A/P (volts/cm/mm)	a (cm)	Average $\int_0^a \alpha dx$ of all gaps	Average exp $[\int_0^a \alpha dx]$ of all gaps
			Dry air—focal length of points 0.009 and 0.019 cm				
1	0.009	6124	14.4×10^4	190.0	0.0462		
1	0.019	8010	10.6×10^4	151.0	0.0740	$f=0.009$	$f=0.009$
2	0.009	6809	14.0×10^4	189.0	0.0446	11.00	59,900 ions
2	0.019	9425	10.6×10^4	152.2	0.0740		
3	0.009	7500	14.3×10^4	189.0	0.0459		
3	0.019	10490	10.9×10^4	153.3	0.0750	$f=0.019$	$f=0.019$
5	0.009	8418	14.8×10^4	194.8	0.0476	12.63	306,000 ions
5	0.019	11234	10.6×10^4	151.6	0.0740		
	0.009	Average	14.30×10^4	190.7	0.0467		
	0.019	Average	10.67×10^4	152.2	0.0742		
			Moist air—relative humidity 55 percent at 20°C				
1	0.009	5925	14.0×10^4	184.0	0.0445		
2	0.009	7300	15.0×10^4	197.5	0.0484	11.00	59,900 ions
3	0.009	7485	14.3×10^4	188.3	0.0458		
5	0.009	8000	14.1×10^4	185.1	0.0448		
		Average	14.3×10^4	188.7	0.0464		

products are all readily ionized by photons from O_2 and N_2. The relative efficiency of photo-ionization by radiations from atoms excited by electron impact in moist and dry air is seen from the values of $\int_0^a \alpha dx$ to be of the order of a factor of 2.

(2) Pre-Onset Streamers

Table II gives the quantitative results obtained for this phenomenon. The effect of moist air of 55 percent relative humidity upon streamer onset was tried for the case of the smaller point. Very little difference was found between the values for dry and moist air. The average of the onset fields at the point surface for all four gaps was 14.3×10^4 volts/cm in moist air as well as in dry air. Slightly more variation between values for different gaps was observed in the case of moist air, as can be seen in Table II. It was found that increasing the relative humidity above 60 percent at 20°C brought in more discrepancies for the onset fields of streamers. These discrepancies are doubtless due to the antagonistic actions of the increased photo-ionization following streamer formation and the rapid attachment of electrons to form ions with water vapor. The water vapor ions will have lower mobilities, and this effective lowering of ionic mobility will critically impede streamer formation.

Test of Meek's Theory

According to Meek's theory, the criterion for streamer formation at the positive electrode is that the radial field about the positive space charge in an electron avalanche attains a value X_1, equal to KX_A; X_A is the field at the electrode surface, and K has a value between 0.1 and 1.0. The radial field X_1, in the case of a uniform applied field X, was predicted by Meek to be given by the relation,

$$X_1 = 5.28\times10^{-7}\frac{\alpha \exp[\alpha x]}{(x/P)^{\frac{1}{2}}} \text{ volts/cm.} \quad (2)$$

In the case of confocal paraboloids, however, we are considering a non-uniform applied field, so

TABLE III. Values for pre-onset corona streamers in dry air showing comparison of experimental results with those calculated from Meek's equation.

Gap δ (cm)	f (cm)	L.H.S.	R.H.S.	Difference L.H.S.-R.H.S.	V from Meek's equation (volts)	V Measured (volts)	Deviation* (%)
1	0.009	18.95	19.27	−0.32	6197	6124	+1.20
1	0.019	19.62	19.16	+0.46	7928	8010	−1.03
2	0.009	18.19	19.13	−0.94	7006	6809	+2.90
2	0.019	19.68	19.16	+0.52	9295	9425	−1.40
3	0.009	18.80	19.17	−0.37	7537	7500	+0.50
3	0.019	19.98	19.18	+0.80	10273	10490	−2.10
5	0.009	19.83	19.23	+0.60	8266	8418	−1.80
5	0.019	19.53	19.16	+0.37	11149	11234	−0.80

* (V calculated $-V$ measured)/V measured.

TABLE IV. Values for onset of steady burst corona.

Gap δ (cm)	(cm)	V (volts)	X_A (volts/cm)	X_A/P (volts/cm/mm)	a (cm)	Average $\int_0^a \alpha dx$ for all gaps	Average $\exp[\int_0^a \alpha dx]$ for all gaps
			Dry air—focal length of points 0.009 and 0.019 cm				
1	0.009	6300	14.9×10^4	195.0	0.0474		
1	0.019	9240	12.3×10^4	175.3	0.0855	$f=0.009$	$f=0.009$
2	0.009	7450	15.3×10^4	201.3	0.0496	13.99	1.19×10^6 ions
2	0.019	10902	12.3×10^4	176.0	0.0885		
3	0.009	8300	15.9×10^4	208.8	0.0517		
3	0.019	11958	12.4×10^4	175.0	0.0880	$f=0.019$	$f=0.019$
5	0.009	9650	16.9×10^4	222.4	0.0559	18.87	128.3×10^6 ions
5	0.019	13663	12.8×10^4	183.6	0.0922		
	0.009	Average	15.75×10^4	206.9	0.0512		
	0.019	Average	12.45×10^4	177.5	0.0886		
			Moist air—relative humidity 65 percent at 20°C				
1	0.009	6700	15.8×10^4	207.0			
2	0.009	8030	16.5×10^4	217.0			
3	0.009	8700	16.6×10^4	219.0			
5	0.009	10200	17.9×10^4	235.0			

that α is not constant with distance x from the point. The radial field for this case is given by the equation,

$$X_1=5.28\times10^{-7}\frac{\alpha_A \exp\left[\int_0^a \alpha dx\right]}{(a/P)^{\frac{1}{2}}} \text{ volts/cm.} \quad (3)$$

α_A is the value of α at the point electrode surface, and corresponds to the applied field X_A; a is the distance of the point of origin of the avalanche from the point. The point of origin of the avalanche may be taken as that point where $\alpha=1$, for in the highly divergent fields the rate of decline of α is so rapid that there is little contribution[11] to the term $\int \alpha dx$ beyond the point where $\alpha=1$. If we put $X_1=KX_A=0.1X_A$, we obtain the equation

$$\int_0^a \alpha dx+\log_\epsilon \alpha_A=12.16 +\log_\epsilon\left(\frac{X_A}{P}\right)+\tfrac{1}{2}\log_\epsilon (Pa). \quad (4)$$

With calculations made on the basis of results for streamer onset, it is possible to check the validity of this equation and thus Meek's criterion for streamer formation. The experimental potentials at different gap lengths and from them the values of the fields X_A [by Eq. (1)] at the point surface for streamer onset enable us to determine $\int_0^a \alpha dx$, α_A, and a for each case. It is important to note here that the values of α come from Sanders' and Townsend's independent determinations and not from corona investigations. The method of calculating the potential for streamer onset is to choose some potential as a possible proper value. The value of the field at the point surface and other values of the field associated with finite values of x are then calculated by means of Eq. (1). By use of Sanders' and Townsend's data, a curve relating α and x is plotted and $\int_0^a \alpha dx$ is determined by graphical integration. $\int_0^a \alpha dx$ is then inserted in Eq. (4) together with the corresponding values of X_A, α_A, and a. If the equation is not satisfied, another potential is chosen and the new values of $\int_0^a \alpha dx$, etc., are inserted in the equation. This process is repeated until sufficient values are obtained to plot a curve relating (L.H.S.*$-$R.H.S.†) with potential V and the value of V is found at which (L.H.S.$-$R.H.S.) is equal to zero. The values of L.H.S. and R.H.S. for the various gaps and the two points used are given in Table III. The equation is seen to be closely satisfied. In the extreme right-hand column of Table III, a comparison is made between the measured potential and that calculated from Eq. (4).

In his original theory, Meek chose the empirical condition that $K=1.0$. Loeb, in reviewing the

* Left-hand side of Eq. (4).
† Right-hand side of Eq. (4).

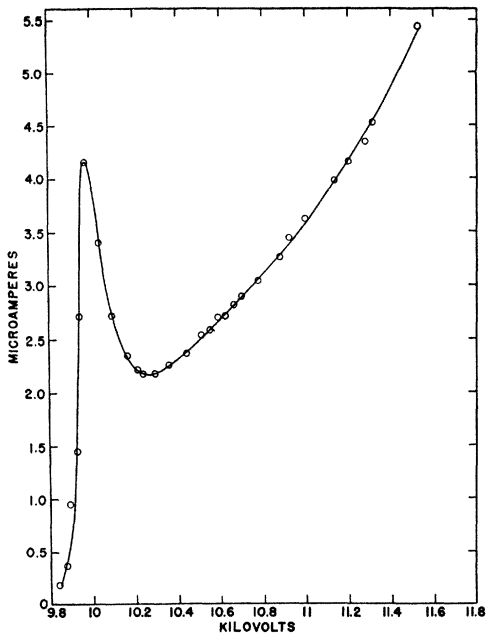

FIG. 2. Corona current-potential curve plotted over the potential range from onset to slightly beyond the linear portion of steady burst corona in air of 65 percent relative humidity at 20°C. Gap length 2 cm; focal length of point 0.0216 cm.

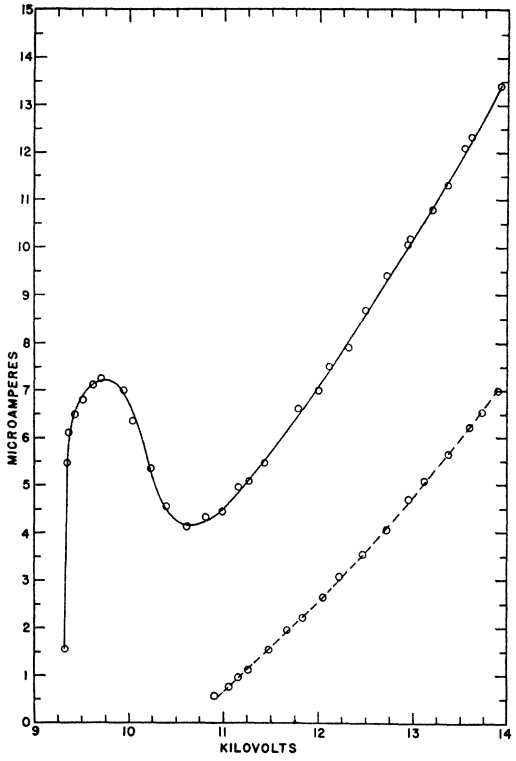

FIG. 3. Corona current-potential curves plotted over the potential range from onset to slightly beyond the linear portion of steady burst corona, showing the effect of gap ventilation. The full curve represents the case of a poorly ventilated gap; the dotted curve was obtained with the same gap well ventilated. Gap length 2 cm; point focal length 0.019 cm.

theory, indicated that K should more likely be less. Meek's calculations with $K=1.0$ gave values of the sparking potential in rough agreement with accepted earlier values. Later studies of the values for breakdown of diverse gaps, as given in the literature, convinced Meek that the value $K=1.0$ was too high, and indicated that a value of $K=0.1$ would be more nearly correct. This became more evident when redeterminations of the sparking potential in air for a 1.0-cm gap by Haseltine[13] yielded the value of 31.6 kilovolts, conforming with some other recent results, in contrast to the older value of 32.2 kilovolts corresponding to $K=1.0$. Because of the accurate determinations of fields possible with confocal paraboloids and the fact that the onset of streamers in corona, as found in the author's investigation, occurred at fields such that Meek's equation yielded the streamers in agreement with theory for $K=0.1$, we must conclude that 0.1 is near the proper value for K.

The fact that we can take values of α from Sanders' data together with the value of K as given by sparking in a plane parallel gap, and predict the streamer onset by Meek's equation, lends strong support to the streamer theory of spark discharge evolved by Loeb and Meek.

[13] W. R. Haseltine, Phys. Rev. **58**, 188 (1940).

(3) Steady Burst Corona

The numerical values associated with the onset of steady burst corona are given in Table IV. Moist air, up to 55 percent relative humidity, had little effect upon the onset fields for steady corona. An interesting result was observed, however, at relative humidities above 60 percent. With a potential on the point corresponding closely to that for the onset of steady burst corona in dry air, there is established a noisy brush corona with the oscillograph showing a rapid succession of very intense streamer pulses. Current measurements, at this part of the observation, indicate a very rapid rise of rather

unsteady current as the potential is increased. Figure 2 illustrates the current-potential relation for this phenomenon. The current soon reaches a peak value and then drops less rapidly toward a minimum with further increase of potential. At the minimum current after onset the oscillograph indicates very few streamers, and with further increase of potential the current begins to rise steadily and linearly with no streamers indicated by the oscillograph. Instead, there is observed the same disturbance as is seen at the onset of steady burst corona in dry air. The data for this curve were taken with a point of 0.0216-cm focal length in conjunction with a 2.0-cm gap; but it is characteristic in general of all the points and gaps that were used. The peak value of current and the potential range from the beginning of any current at all to the start of steady burst corona are very sensitive to changes in humidity. It was impossible to maintain humidity constant enough, with the available apparatus, to get exact reproduction of results. It is to be noted that the potential range, wherein this unsteady brush type corona occurs, is quite limited; consequently, if an observer is changing the potential in steps of 100 volts or more, this unusual part of the curve may be missed entirely. The lower part of Table IV gives the potentials and corresponding approximate fields for the establishment of *steady* burst corona with various gaps; using the 0.009-cm focal length point in moist air of approximately 65 percent relative humidity at 20°C. The fields at the point for the different gaps do not agree with each other as well as in the case of dry air and of course are all higher. This disagreement can be explained by the extreme sensitiveness of the range of brush corona potential to slight humidity changes. The effect of moisture at corona onset is not entirely clear, but a possible explanation is that it increases photoelectric ionization so greatly that streamers can propagate and may take the place of bursts while the current rises rapidly. Furthermore, when the ionization products get loose in moist air, space charges rapidly become very large, and the result of this abnormally rapid space charge fouling is a drop in current until the potential increases to a value where the applied fields can clear out the space charges.

A similar effect upon the current-potential curves in dry air was observed with a poorly ventilated gap. Comparative curves for poor and good ventilation are shown in Fig. 3. This effect is undoubtedly due to the formation of nitric oxides, which are produced in considerable quantities, and have ionization thresholds in the ultraviolet around 1200 angstroms and above. Thus, as in the case of moist air, increased photoelectric ionization may allow streamers to propagate and take the place of bursts with a resulting abnormal rise in current, but, in addition, the oxides can produce very large space charge effects through attaching electrons and slowing both positive and negative ions; so that the current eventually drops until sufficient fields are applied to remove the space charges. With dry air and a well ventilated gap, the current-potential curves have the same general characteristics as those obtained by Kip[4] with point-to-plane corona.

(4) Spark Breakdown

The breakdown potentials and the corresponding but approximate fields calculated from them are tabulated in Table V. Field curves, obtained by assuming no space charge effects, are shown in Fig. 4. These curves, of course, do not represent the exact state of affairs because of the field distorting charges which, with heavy currents, must exist in the gap. Nevertheless, it is easy to see that the gap length has a decided effect upon the fields for breakdown.[4] Pre-onset

TABLE V. Values for breakdown potentials and approximate fields.

Gap δ (cm)	f (cm)	V (volts)	X (volts/cm)	X/P (volts/cm/mm)
		Dry air		
1	0.009	12000	28.3×10^4	372
1	0.019	13220	17.6×10^4	252
2	0.009	17500	36.0×10^4	474
2	0.019	22889	25.9×10^4	370
3	0.009	23400	44.7×10^4	588
3	0.019	29053	30.2×10^4	425
5	0.009	35000	61.3×10^4	807
5	0.019	42092	39.7×10^4	567
		Moist air—relative humidity 55 percent at 20°C		
1	0.009	11200	26.4×10^4	347
2	0.009	18000	37.0×10^4	487
3	0.009	23340	44.6×10^4	587
5	0.009	35000	61.3×10^4	807

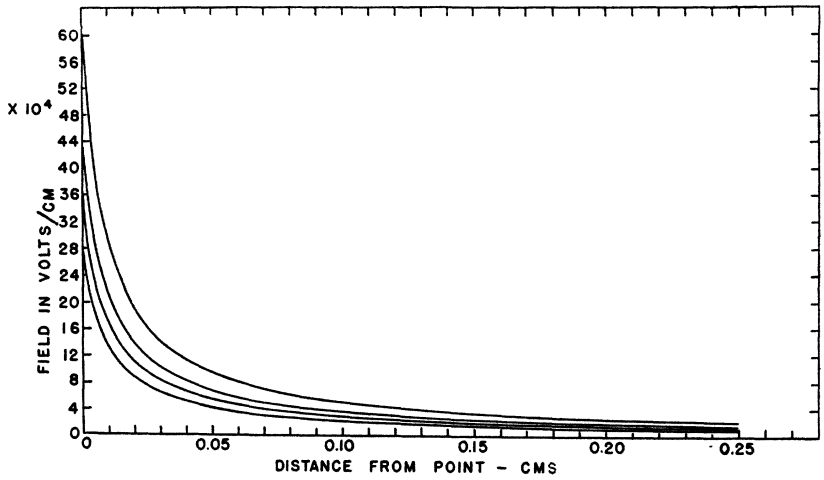

FIG. 4. Breakdown field *vs.* distance from point for various gaps. Beginning with the bottom curve for the 1-cm gap, the curves for the 2-, 3-, and 5-cm gaps follow above in the order of the gap lengths.

bursts, streamers, and steady burst corona each start, for a given point, when the field at its surface reaches a value unique for the phenomenon. Furthermore, the field throughout the gap for any gap is the same within the limits of the gap. There is thus one value of $\int_0^a \alpha dx$ for each phenomenon and each point at which the phenomenon begins. $\int_0^a \alpha dx$ is independent of gap length because the lower limit ($\alpha = 1$) occurs too near the point (i.e. $a < 1$ cm). The field for breakdown, with a given gap, is not independent of gap length since streamers must cross the gap for breakdown to occur; and the shorter it is the more easily do streamers cross because, (1) space charges are cleared more readily, (2) the streamers do not have so far to go.

From Table V it is seen that the effect of moist air is of no consequence except for the shortest gap. With relative humidities above 65 percent, however, breakdown may occur at lower potentials and the results are less reproducible. It was found that poor circulation of air in the gap had a more profound effect upon the breakdown potential than did water vapor; and it is quite likely that the experimental difficulty in properly ventilating the 1.0-cm gap resulted in the comparatively low value for breakdown potential when air of 55 percent relative humidity was used. It was observed consistently that, with either moist or dry air, breakdown would occur at lower potentials when the gap was poorly ventilated. For example, in the case of a 2.0-cm gap with a point of 0.019-cm focal length, breakdown occurred at 16,678 volts with poor ventilation, but increased to 22,889 volts with good ventilation.

In conclusion, the writer takes this opportunity to express his gratitude to Professor Leonard B. Loeb at whose suggestion this work was undertaken, and whose hearty support in guidance and interpretation of results have been most helpful.